JCTC Journal of Chemical Theory and Computation

ARTICLE

pubs.acs.org/JCTC

Chemiluminescence and Fluorescence States of a Small Model for Coelenteramide and Cypridina Oxyluciferin: A CASSCF/CASPT2 Study

Daniel Roca-Sanjuán,*[,†] Mickael G. Delcey,[†] Isabelle Navizet,[‡] Nicolas Ferré,[§] Ya-Jun Liu,[∥] and Roland Lindh*[,†]

[†]Department of Chemistry—Ångström, Theoretical Chemistry Programme, Uppsala University, P.O. Box 518, S-75120 Uppsala, Sweden

[‡]Molecular Science Institute School of Chemistry, University of the Witwatersrand, PO Wits Johannesburg 2050, South Africa

[§]Universités d'Aix-Marseille I, II, et III-CNRS UMR 6264: Laboratoire Chimie Provence, Equipe: Chimie Théorique Faculté de St-Jérome, Case 521, 13397 Marseille Cedex 20, France

[∥]Key Laboratory of Theoretical and Computational Photochemistry, Ministry of Education, College of Chemistry, Beijing Normal University, Beijing 100875, China

Supporting Information

ABSTRACT: Fluorescence and chemiluminescence phenomena are often confused in experimental and theoretical studies on the luminescent properties of chemical systems. To establish the patterns that distinguish both processes, the fluorescent and chemiluminescent states of 2-acetamido-3-methylpyrazine, which is a small model of the coelenterazine/coelenteramide and Cypridina luciferin/oxyluciferin bioluminescent systems, were characterized by using the complete active space second-order perturbation (CASPT2) method. Differences in geometries and electronic structures among the states responsible for light emission were found. On the basis of the findings, some recommendations for experimental studies on chemiluminescence are suggested, and more appropriate theoretical approaches are proposed.

INTRODUCTION

According to the International Union of Pure and Applied Chemistry (IUPAC) Gold Book,[1] chemiluminescence is the "emission of radiation resulting from a chemical reaction," while fluorescence is the "luminescence which occurs essentially only during the irradiation of a substance by electromagnetic radiation." Both phenomena can be described mechanistically by means of the scheme displayed in Figure 1. In the fluorescence process, the Franck−Condon structure is relaxed upon light absorption toward a minimum energy point in the excited state. From this *fluorescent state* (FS), the molecule emits radiation. The general picture for the chemiluminescence reaction mechanism, as established nowadays, is the following: (1) The reactants reach the transition state (TS) via a thermal movement, for example, in peroxo compounds, increasing mainly the OO bond distance. (2) A region of near-degeneracy or a conical intersection (CI) seam between the ground and excited state follows, promoting the system to the electronically excited hypersurface—the formation of a stable intermediate in this step is possible—and (3) the molecule decays from the *chemiluminescence state* (CS) to the ground state by means of light emission.[2−5] Both fluorescent and chemiluminescent processes imply the emission of light from an excited state of the system. However, as we prove in this contribution, they correspond to different phenomena, and the excited state responsible for the emission of radiation are not necessarily the same.

Chemiluminescence and bioluminescence phenomena—the latter corresponding to the luminescence taking place in a living organism—have attracted much experimental and theoretical attention not only as a subject of academic interest in the field of biochemistry but also in the development of luminescence-based analytical techniques and the design of energy saving materials, where the chemical properties of chemiluminescent or bioluminescent systems are taken into account.[6−8] Since the first appearance in 1968 of a monograph focused exclusively on the topic,[9] many experimental results have been published, showing

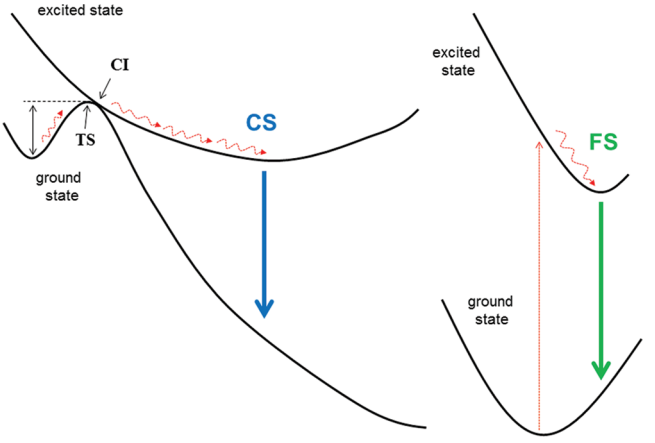

Figure 1. General scheme of the chemiluminescence (left) and fluorescence (right) processes. The chemiluminescence (CS) and fluorescence (FS) states are illustrated. The transition state (TS) and conical intersection (CI) points related to the former phenomenon are also shown.

Received: July 8, 2011
Published: November 02, 2011

ACS Publications © 2011 American Chemical Society

a large list of chemiluminescent autoxidation and bioluminescent, enzyme-catalyzed, reactions (see for instance refs 10 and 11). A common pattern of some of these chemiluminescent reactions and almost all of the luminescent processes taking place in living organisms is the formation and decomposition of a molecule containing a peroxo intermediate, either 1,2-dioxetane or 1,2-dioxetanone (hereafter dioxetanone), resulting in the formation of a species in the excited stated which emits light. Much effort has been focused on understanding the mechanism in small molecules containing these structures. Lindh and coworkers have been carrying out over the past five years a series of complete active space second-order perturbation (CASPT2) studies on the decomposition of 1,2-dioxetane and dioxetanone.[2,3] A two-step mechanism was found in both cases. First, a biradical intermediate is formed through a TS, which is characterized by an OO stretching (dioxetanone) or a combination of OO stretching and OCCO torsion (1,2-dioxetane). The subsequent cleavage of the CC bond can bring the system to the excited state responsible for light emission. Meanwhile, differences at the molecular level were found in the study of a thiazole-substituted dioxetanone containing a π electron-donating group. This small model of the firefly luciferin molecule was employed to analyze the chemiluminescence reaction by means of the CASPT2 method.[4] According to these results, and in agreement with other density functional theory (DFT) studies[12] with molecules containing the dioxetanone moiety coupled to an electron-donating group, a concerted charge transfer induced luminescence (CTIL) mechanism takes place. The electron-donating group, with a low ionization potential, partially delocalizes the π-electron toward the dioxetanone moiety, via the π system, decreasing the energy barrier of the reaction and enhancing the efficiency of the luminescence.

Reliable predictions of the whole chemiluminescent/bioluminescent mechanism require finding the point on the potential energy surface (PES) where the excited state can be populated efficiently and following the reactivity in this electronically excited PES. Modern computational chemistry offers several methods for describing electronically excited states of small to medium-size systems. However, the accurate prediction of excited electronic states in large-size systems is still a challenge, although many improvements are currently explored in the CASPT2 method to enable applications to large systems.[13] Therefore, different approximations have been employed in the theoretical studies on chemiluminescence and bioluminescence. A commonly used strategy, which avoids following the photoreactivity in the excited state, is to characterize the path toward the TS of the luminescent reaction before the nonadiabatic crossing (see Figure 1) by means of the DFT method and, next, make use of the Time-Dependent DFT (TD-DFT) and configuration interaction singles (CIS) methodologies to model the properties of the excited state around the region of the equilibrium structure for the product of the thermal decomposition reaction. Several imidazo[1,2-*a*]pyrazin-3(7*H*)-one (imidazopyrazinone) derivatives and dioxetanone-containing molecules with a substituent of low oxidation potential have been studied by using this approach.[12,14] In other cases, charge-transfer excitations over the π-conjugated system of the reaction product are used to extract conclusions about the concerted CTIL mechanism, although the CTIL is the excitation to the antibonding-σ orbital of the OO bond in the dioxetanone moiety, which facilitates the decomposition of the molecule by lowering the activation energy required for bond breaking.[15]

On the other hand, several experiments were designed in the past to study the chemiluminescence properties of different molecular systems by irradiating the spent solution after chemiluminescence and measuring the spectrum of the radiation emitted, or directly by studying the fluorescent properties of the final products, such as distinct phenolate anions of coelenteramide analogues.[16−18] Other experimental determinations of the light-emitting species are based on matching the chemiluminescence spectrum with the fluorescence. Examples can be found in the studies on the coelenterazine/coelenteramide[19,20] system, or the luciferin/oxyluciferin molecules from the *Cypridina* (Vargula)[21] and firefly[22] organisms. Indeed, the bioluminescence and fluorescence spectra show noticeable differences, as was proved by Belogurova et al. through the deconvolution of the bioluminescence spectra of photoproteins from marine coelenterates and the photoluminescence spectra of the bioluminescent reaction products.[23] These differences are commonly assigned to different forms of the product [nonionized, amide, ion-pair proton transfer, phenolate, pyrazine-N(4) anion forms].

Care must be taken with both mentioned experimental and theoretical procedures, since the region reached on the excited-state surface need not correspond in general to the structure responsible for light emission in the chemiluminescence or bioluminescence processes. To establish the molecular basis of the differences between both luminescent phenomena, we employed 2-acetamido-3-methylpyrazine. This molecule is similar to the product of decomposition of other imidazopyrazinone compounds reported in the literature[14] and corresponds to a small model of coelenteramide and *Cypridina* oxyluciferin, which are the light-emitting species present in some marine bioluminescent organisms, such as the hydromedusa *Aequorea*[24] and the hydroid *Obelia*,[25] in the first case, and the ostracod *Vargula hilgendorfii*,[26] in the latter (see Figure 2). The bioluminescent process in these organisms involves the protein systems aequorin, obelin, and *Cypridina* luciferase, respectively, which are formed by the apoprotein, coelenterazine (in the two former) or *Cypridina* luciferin (in the latter), and molecular oxygen. These complexes emit blue light through an intramolecular reaction, decomposing into apoprotein, coelenteramide (in aequorin and obelin) or *Cypridina* oxyluciferin (in *Cypridina* luciferase), and CO_2.[24] The present study will contribute to the understanding of the bioluminescent properties of the coelenterazine/coelenteramide and *Cypridina* luciferin/oxyluciferin systems. Since there is a controversy over the protonation state of the light-emitting species,[27] both anion and neutral forms were considered. The characterization of the CS and FS states was carried out by means of the CASPT2 method, finding relevant differences at the molecular level.

METHODS AND COMPUTATIONAL DETAILS

The double-ζ ANO-S[28] basis set with a contraction scheme [3s2p1d] for carbon, oxygen, and nitrogen atoms and [2s1p] for hydrogen (i.e., the ANO-S-VDZP basis set) was used throughout. Geometry optimizations, minimum energy reaction paths (MEPs), and the determination of surface crossings were carried out at the complete active space self-consistent field (CASSCF) level of theory with no symmetry restriction (C_1 symmetry), and the energies of the single points were corrected including the second-order perturbation treatment (CASPT2).[13,29] In some cases, geometry optimizations were performed at the CASPT2 level, by using numerical gradients, to analyze the effect of the

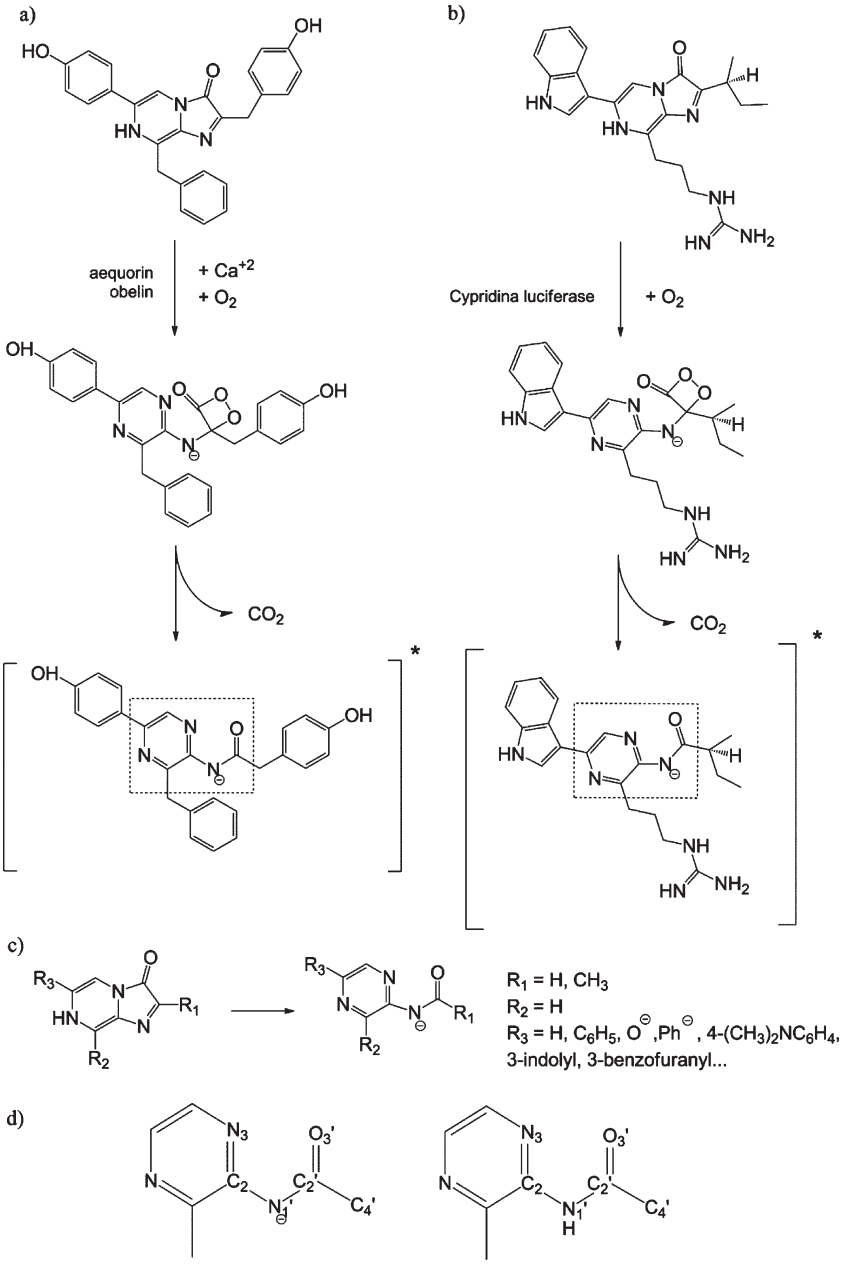

Figure 2. Bioluminescence reactions in the coelenterazine/coelenteramide (a) and *Cypridina* luciferin/oxyluciferin (b) systems. Two steps are represented: (1) The peroxo intermediate is produced from the reaction between coelenterazine (a) or *Cypridina* luciferin (b) and molecular oxygen in the aquorin/obelin (a) or *Cypridina* luciferase (b) proteins; (2) the peroxo intermediate decomposes, creating coelenteramide (a) or *Cypridina* oxyluciferin (b) in the excited state. (c) Distinct imidazo[1,2-*a*]pyrazin-3(7*H*)-one (imidazopyrazinone) derivatives employed in the experimental and theoretical studies on the bioluminescence and chemiluminescence of coelenterazine/colenteramide and *Cypridina* luciferin/oxyluciferin (left) and the product of the chemical reaction (right). (d) Chemical structure of the anionic (left) and neutral (right) small models studied in the present contribution with the labels used in the text.

dynamical correlation in the geometries and the reliability of the equilibrium structures that were obtained with the noncorrelated CASSCF method. MEPs were built as steepest descendent paths in which each step requires the minimization of the PES on a hyperspherical cross-section of the PES centered on the initial geometry and characterized by a predefined radius.[30] Mass-weighted coordinates were used; therefore the MEP coordinate corresponds to the so-called intrinsic reaction coordinate (IRC), measured in atomic units, that is, bohr·amu$^{1/2}$. The CI was computed by using the restricted Lagrange multipliers technique as included in the MOLCAS-7.6 package,[31] in which the lowest-energy point was obtained under the restriction of degeneracy between the two considered states.[30] In all of the CASPT2 calculations, the core orbitals of non-hydrogen atoms were not correlated, an imaginary level-shift of 0.2 au was turned on a priori to minimize weakly interacting intruder states, and the nonstandard IPEA modification of the zeroth-order Hamiltonian with a value of 0.00 au was employed. The ANO-S-VDZP basis set and nonstandard IPEA are commonly used in studies on photoreactivity (see, for instance, González-Ramírez et al.[32] and

Table 1. Vertical Absorption Energies (in eV) and Oscillator Strengths (f) for the Anionic System of 2-Acetamido-3-methylpyrazine

transition	ΔE	f
$\pi_{HOMO} \rightarrow \pi_{LUMO}^*$	3.25	0.113
$\pi_{HOMO} \rightarrow \pi_{LUMO+3}^*$	4.03	0.436
$\pi \rightarrow \pi^*$	5.03	0.068
$\pi_{HOMO} \rightarrow \pi_{CO}^*$ (CTIL)	7.19	0.056

Table 2. Vertical Absorption Energies (in eV) and Oscillator Strengths (f) for the Neutral System of 2-Acetamido-3-methylpyrazine

transition	ΔE	f
$\pi_{HOMO} \rightarrow \pi_{LUMO}^*$	4.27	0.066
$\pi_{HOMO} \rightarrow \pi_{LUMO+3}^*$	5.14	0.222
$\pi \rightarrow \pi^*$	6.04	0.061
$\pi_{HOMO} \rightarrow \pi_{CO}^*$ (CTIL)	7.24	0.152

references therein). Further test calculations were carried out with the ANO-RCC type of basis set or the standard IPEA (0.25 au), as used in previous studies on chemiluminescence,[3,4] and they do not change the conclusions.

Two sets of active spaces were used in the CASSCF models (see Figures S1 and S2, Supporting Information). In order to characterize the chemiluminescent and fluorescent properties of the molecules, an optimal candidate for the calculations is an active space of 10 electrons distributed in nine orbitals [denoted as CAS(10-in-9)]. All of the π orbitals of the six-member-ring, $N_{1'}$ atom, and carbonile group are considered in this case. It has been shown elsewhere that a lone pair of the oxygen atom may be relevant to the chemiluminescent reactivity.[3,4] Therefore, an active space including this orbital [CAS(12-in-10)] was also employed for the calculations related to the chemiluminescent state.

All of the computations were carried out by using the MOLCAS 7.6 quantum-chemical software.[31]

RESULTS AND DISCUSSION

Fluorescence State (FS). The CASPT2 vertical spectra of the anionic and neutral molecules computed at the minimum structure of the ground state [hereafter $(S_0)_{min}$] are compiled in Tables 1 and 2, respectively, and the shapes of the natural orbitals (NOs) involved in the most relevant excitations are depicted in Figure 3. The lowest-lying excited states (S_1 and S_2) are related in both molecules to the same transitions between NOs delocalized over the π-aromatic system. While S_1 can be characterized by an excitation from the highest occupied to the lowest unoccupied molecular orbitals (HOMO and LUMO, respectively) from the previous self-consistent field (SCF) calculation, the HOMO and LUMO+3 orbitals are involved in S_2 (see Figure 3 and Tables 1 and 2). S_2 has the highest oscillator strength (f), and therefore will be the most populated state upon irradiation. Lower energies are required to excite the anionic system. In particular, the brightest state of the anion requires 4.03 eV, and the lowest-energy state appears at 3.25 eV, while the corresponding transitions in the neutral system are located more than 1 eV higher in energy at 5.14 and 4.27 eV, respectively. Direct comparisons with the experimental absorption

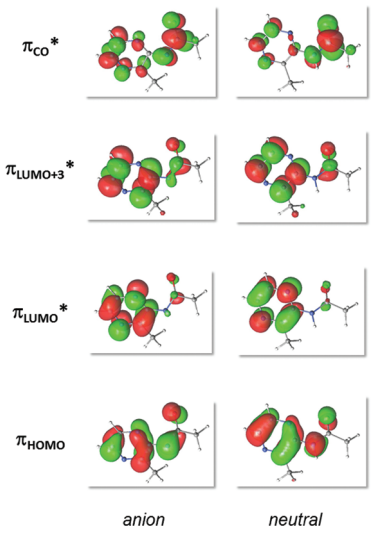

Figure 3. Selected natural orbitals (NOs) to analyze the absorption and emission properties of the anionic and neutral systems of 2-acetamido-3-methylpyrazine (see text). The complete sets of NOs present in the active space of the CASSCF/CASPT2 calculations can be found in Figures S1 and S2 (Supporting Information).

spectra of coelenteramide are difficult since the transitions will be mainly affected by the phenolate substituent of the pyrazine ring (see Figure 2). Nevertheless, two peaks are also found in different coelenteramide analogues studied by Shimomura and Teranishi.[18] As explained above and proved in several studies,[4,12] efficient chemiluminescent systems are governed by a charge-transfer excitation from an electron-donating part of the molecule to the dioxetanone moiety (concerted CTIL mechanism). In the systems studied here at the Franck–Condon geometry, none of the lowest excited states are characterized by a CTIL excitation, even in the anion species in which the $N_{1'}$ atom is charged negatively, and therefore the system presents a lower oxidation potential.[12] To find a state with charge-transfer character to the carbonile group, more than 10 roots are needed in the State Averaged CASSCF (SA-CASSCF) wave function. These transitions correspond to excitations from the SCF HOMO to the π^* orbital located mainly in the CO group (see Figure 3) and require energies larger than 7 eV (see Tables 1 and 2). According to these results, the states with CTIL character, which are involved in the chemiluminescence phenomenon, are not accessible at the optimized geometry of the ground state of 2-acetamido-3-methylpyrazine anion and neutral molecules.

The minima of the S_1 and S_2 states for the anion and neutral molecules were subsequently determined by means of the CASSCF/CASPT2 method to analyze the fluorescent properties of these systems. A minimum point in the PESs of the S_2 state is found relatively close in energy to the S_1 surface (0.29 eV higher), with a vertical emission to the ground state (VE) of 2.39 eV and a f of 0.001, while the S_1 geometry optimization results in a structure with a VE of 2.13 eV and a larger f (0.043), see Table 3. In the neutral molecule, the equilibrium structures have higher VEs, similarly to the results found in the absorption computations. In particular, S_2 and S_1 present a VE of 2.75 and 4.07 eV, respectively, with a higher probability of fluorescence from the latter (the f values are 0.001 and 0.046, respectively). The theoretical description of the fluorescence process in the anionic

Table 3. Vertical Emission Energies (in eV) and Oscillator Strengths (f) for the Anionic System of 2-Acetamido-3-Methylpyrazine in the Fluorescence (FS) and Chemiluminescence (CS) States[a]

		ΔE	f
fluorescence	$(S_1)_{min}$	2.11	0.040
	$(S_2)_{min1}$	3.59	0.261
	$(S_2)_{min2}$	2.21	0.001
chemiluminescence	CS_{10in9}	2.59	0.006
	CS_{12in10}	1.72	0.002
	CS_{caspt2}	1.60	0.139

[a] Fluorescent minima computed at the CASPT2//CASSCF(10-in-9) level of theory and chemiluminescence states obtained with different CASSCF/CASPT2 approaches (see text).

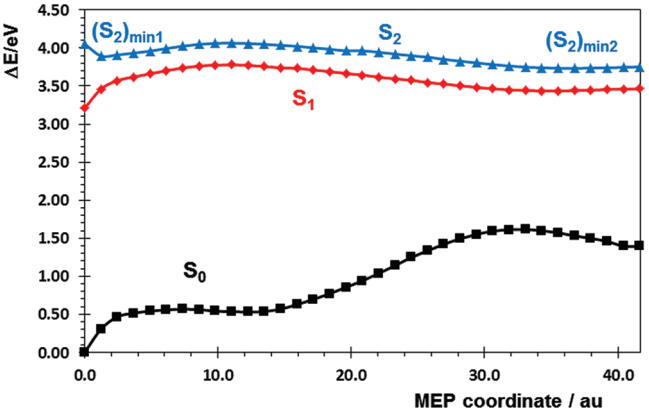

Figure 4. Low-lying singlet states of the 2-acetamido-3-methylpyrazine anion computed at the CASPT2//CASSCF level along the minimum energy path (MEP) of the S_2 state from the ground-state minimum. The S_2-MEP ends in the equilibrium geometry of $(S_2)_{min2}$.

molecule was later improved by using the photochemical reaction path approach[33] to characterize with accuracy the emissive state of the molecule. The anion form of 2-acetamido-3-methylpyrazine is expected to be more relevant in the chemiluminescence, as the system has a better electron-donating component, and therefore a more exhaustive analysis is necessary. A MEP from the brightest state, S_2, was performed (S_2-MEP); Figure 4 displays the CASPT2 energies for the low-lying S_0, S_1, and S_2 states along the S_2-MEP. The CASSCF S_2-MEP (see Figure S3, Supporting Information) ends up in the region of the previously optimized minimum on the S_2 surface, and two minima are found when the dynamical correlation is included through the CASPT2 [hereafter, $(S_2)_{min1}$ and $(S_2)_{min2}$], as can be seen in Figure 4. The structure $(S_2)_{min1}$, which is found close to the ground-state minimum geometry, has a VE of 3.59 eV and a high probability of fluorescence (f = 0.261). This minimum is however very shallow, and from the Franck−Condon structure the system can surmount the energy barrier of 0.16 eV and reach the second minimum $(S_2)_{min2}$. The stability of this structure, $(S_2)_{min2}$, is also relatively small, since the S_1 surface is only 0.29 eV lower and a CI between both states is found energetically close to $(S_2)_{min2}$, in particular, only 0.16 eV above this minimum. From this CI, a MEP was computed on the PES of the S_1 state (S_1-MEP) to study the evolution of the system after reaching the crossing point between both S_1 and S_2 surfaces (see Figure 5 and

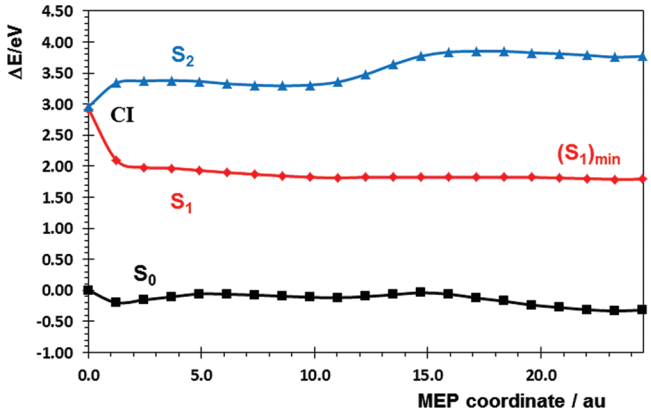

Figure 5. Low-lying singlet states of the 2-acetamido-3-methylpyrazine anion computed at the CASPT2//CASSCF level along the minimum energy path (MEP) of the S_1 state from the conical intersection between the S_2 and S_1 states (CI). The S_1-MEP ends in the equilibrium geometry of $(S_1)_{min}$.

Figure S4, Supporting Information). The S_1 minimum previously optimized at the CASSCF level [hereafter, $(S_1)_{min}$] is reached at the end of the S_1-MEP. As can be seen in Figure 4, S_1 and S_2 states are close in energy (<0.3 eV) over a large region of the MEP, which implies a high probability of hopping between the S_1 and S_2 surfaces. In order to investigate alternative photochemical paths that may occur and therefore to further characterize the fluorescent properties of the 2-acetamido-3-methylpyrazine anion, several geometry optimizations and a MEP were computed on the S_1 surface from different points of the S_2-MEP. According to the computations of the f magnitude, the optical interaction between the S_2 and S_1 states decreases toward the CI. Thus, the MEP was performed from the equilibrium geometry $(S_2)_{min1}$ (see Figures S5 and S6, Supporting Information). All of these computations arrive at the same point, $(S_1)_{min}$, suggesting that other structures are not relevant in the fluorescence of the molecule. In addition, since S_1 can also be populated after irradiation (see the value for f in Table 1), the evolution of this state from the Franck−Condon point was also characterized by means of a MEP (see Figures S7 and S8, Supporting Information). Again, the structure of $(S_1)_{min}$ is reached at the end of the computation.

Figure 6 displays the energy profile of the photochemical paths analyzed. All three minima found will contribute in some extent to the fluorescence of the system. $(S_2)_{min1}$, even with a large f, is a shallow minimum, and a large amount of the molecules UV-irradiated will possess enough energy to access the second minimum and the CI and continue deactivating the excess energy toward the $(S_1)_{min}$. Alternative paths derived from the hopping from the S_2 to S_1 surfaces along the region of close energy drive the system to the same emissive state, $(S_1)_{min}$. From this structure, there are no accessible crossings with the ground state, and the system will fluoresce. The experimental emission spectrum of the amide anion form of coelenteramide shows only one fluorescence peak at 2.70−2.85 eV.[18] Probably, it is related to the $(S_1)_{min}$ structure obtained in the present study, although, as explained above, comparisons of the transition energies between coelenteramide and 2-acetamido-3-methylpyrazine are not straightforward.

The analysis of the electronic configuration and the geometrical parameters that are relevant to fluorescence is crucial for

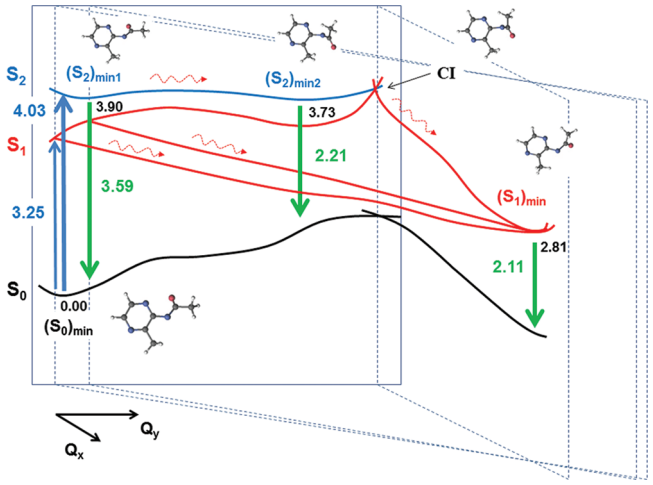

Figure 6. Scheme of the main decay paths on the singlet manifold of the 2-acetamido-3-methylpyrazine anion. Structures for the relevant points in the fluorescence process are shown. The numerical values (in eV) correspond to the vertical absorption (blue) and emission (green) energies computed at the CASPT2//CASSCF level. The Q_y coordinate is mainly related to the rotation of the acetamido group with respect to the methylpyrazine part around the $C_{2'}N_{1'}C_2N_3$ dihedral angle and to the puckering of the six-member ring, whereas Q_x is associated with the orientation of the CO and methyl groups relative to the rest of the molecule.

Table 4. Computed Structural Parameters for the Relevant Geometries in the Absorption and Emission Phenomena of 2-Acetamido-3-methylpyrazine[a]

		CO	$O_{3'}C_{2'}N_{1'}C_{4'}$	$C_{2'}N_{1'}C_2N_3$
literature[b]	Conf1	1.20	−178	−5
	Conf2	1.20	174	173
	Conf3	1.21	179	2
	Conf4	1.20	176	−170
absorption	$(S_0)_{min}$	1.25	−177	36
fluorescence	$(S_1)_{min}$	1.20	−173	4
	$(S_2)_{min1}$	1.23	178	52
	$(S_2)_{min2}$	1.20	−175	92
	CI	1.20	−176	95
chemiluminescence	CS_{10in9}	1.28	−132	3
	CS_{12in10}	1.40	−125	2
	CS_{caspt2}	1.33	−127	20

[a] The reported values for the emissive states of different conformers related to 2-acetamidopyrazine are also shown. Bond lengths are in Å and dihedral angles in degrees. [b] Related geometrical parameters for the lowest excited state optimized structure of four conformers of the 2-methanamidopyrazine molecule computed at the CIS/6-31+G(d) level of theory. Data taken from ref 14.

establishing the fluorescent patterns and distinguishing them from chemiluminescence. Excitations between NOs localized in the six-member ring characterize the electronic changes that govern the photophysics of the systems (see Figure 3). All of the optimized structures and points along the MEPs have this nature. Charge-transfer transitions to the carbonile group are very high in energy, as proved in the computation of the absorption spectrum. To show the structural properties of the FS, the CO bond distance and the $O_{3'}C_{2'}N_{1'}C_{4'}$ and $C_{2'}N_{1'}C_2N_3$ dihedral angles were selected (see Figure 2). The first angle shows out-of-plane distortions of the carbonile group with respect to the adjacent $N_{1'}$ and $C_{4'}$ atoms. Meanwhile, the latter is related to the rotation of the acetamido group with respect to the plane defined by the methylpyrazine moieties. The values obtained for all of the relevant points in the fluorescent study of the 2-acetamido-3-methylpyrazine anionic and neutral systems are compiled in Table 4. The CO bond length for all minima of the anion [$(S_1)_{min}$, $(S_2)_{min1}$, and $(S_2)_{min2}$] are in the range 1.20−1.23 Å. Similar values are obtained in the geometry optimizations of S_2 and S_1 in the neutral species, in particular, 1.20 Å for both minima. These CO bond distances are close to those obtained for the ground-state minimum geometry and correspond to a double bond CO. Regarding the dihedral angles, different values are obtained for $C_{2'}N_{1'}C_2N_3$. As can be seen in Figure 6 and Table 4, this angle increases along the S_2-MEP and reaches the largest value at the CI point where the acetamido group becomes perpendicular to the methylpyrazine moiety. From the CI and along the S_1-MEP, the dihedral angle decreases and ends at a value of 4° in the $(S_1)_{min}$ minimum structure. The behavior of the $O_{3'}C_{2'}N_{1'}C_{4'}$ dihedral angle is different with respect to $C_{2'}N_{1'}C_2N_3$. The former is kept practically unchanged during the fluorescent process, with a value that differs by only 5° from a planar conformation of the carbonile. In the neutral form, out-of-plane distortions are not obtained for neither the S_2 nor S_1 minima. The findings for the CO bond length and $O_{3'}C_{2'}N_{1'}C_{4'}$ dihedral angle show that the fluorescent events are characterized by a double-bond CO and an sp^2 hybridization of the $C_{2'}$ atom, which is in agreement with the fact that the electronic excitations involved do not change markedly the π-bonding character of the carbonile group. The structure of the fluorescence state is therefore far from the geometry of the peroxo intermediate which decomposes to the species responsible for the chemiluminescence, with a single-bond and sp^3 hybridization of the carbonile moiety (see Figure 2).

Chemiluminescence State (CS). The CS is the point on the excited-state PESs reached after the decomposition of the dioxetanone (or peroxo) precursor and is responsible for light emission (see Figure 2). As explained in the Introduction, it is common in the theoretical studies on chemiluminescence to start with the ground-state optimized structure of the reaction product in order to find the CS. This strategy is dangerous, since the molecule reaches the excited state at the region of energy crossing (CI) between the PESs of the ground and excited states in the vicinity of the TS related to the fragmentation reaction (see Figure 1), and the molecular structures at these points are closer to the peroxo intermediate than to the ground-state minimum of the reaction product, as has been proved in CASSCF/CASPT2 studies on the decomposition of 1,2-dioxetane and dioxetanone,[2,3] as well as DFT investigations with coelenterazine/coelenteramide models.[14] From the CI point close to the TS, the photoreactivity continues in the excited state toward the CS. Therefore, a more appropriate strategy to find the CS might be to consider the peroxo molecule, which is the intermediate in the coelenterazine/coelenteramide and *Cypridina* luciferin/oxyluciferin reactions (see Figure 2), as the starting structure in the study.

The ground state of the peroxo intermediate for the anionic and neutral small models of coelenteramide and *Cypridina* oxyluciferin was optimized at the CASSCF level of theory. At these structures, the $C_{2'}$ atom clearly shows sp^3 hybridization (the dihedral angles $O_{3'}C_{2'}N_{1'}C_{4'}$ are around −125° for both systems)

dx.doi.org/10.1021/ct2004758 |J. Chem. Theory Comput. 2011, 7, 4060–4069

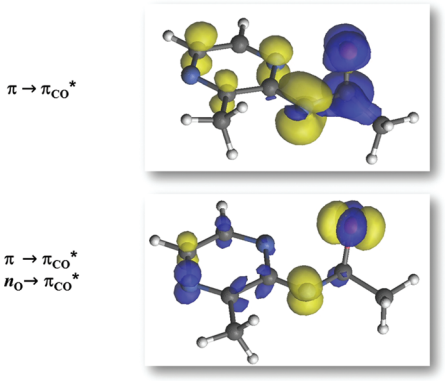

Figure 7. Electron-density difference between the ground and charge-transfer-induced-luminescence (CTIL) states of the peroxo-like form calculated with the CASSCF method and two active spaces: all π orbitals [CASSCF(10-in-9), top] and the π system plus the lone pair orbital n_O in the oxygen atom of the carbonile group [CASSCF(12-in-10), bottom].

and the CO bond lengths are 1.53 and 1.47 Å, respectively. After the removal of the CO_2 moiety, resulting in 2-acetamido-3-methylpyrazine with a structure that will be named "peroxo-like form", the lowest vertical transitions were calculated by means of the CASSCF/CASPT2 method and using only the π MOs in the active space. In contrast to the vertical electronic transitions at the ground-state minimum, the $\pi_{HOMO} \rightarrow \pi_{CO}^*$ (see Figure 3) excitation is present here in the lowest excited state, with a vertical absorption energy of 2.36 eV. The electron-density difference between the lowest excited and ground states is shown in Figure 7. This electronic transition corresponds to the CTIL state, which is characterized by the charge transfer from the π-aromatic system to the CO moiety and is responsible for enhancing the chemiluminescence efficiency.[4,12] None of the lowest excited states of the neutral form with the peroxo-like structure has CTIL character. Thus, the presence of the deprotonated nitrogen (anion system) seems to be necessary in the molecule studied to promote the concerted CTIL mechanism for chemiluminescence. The charged nitrogen activates the electron donation from the π system by lowering the ionization potential of the HOMO.

In order to explore the properties of the PESs in the surroundings of the peroxo-like form, in the crossing region between the surfaces of the ground and excited states, and along the path toward the decomposition product, the electronic structure of the lowest lying excited state and the energy difference between the CTIL ($\pi_{HOMO} \rightarrow \pi_{CO}^*$) and $\pi_{HOMO} \rightarrow \pi_{LUMO}^*$ excited states and between the CTIL and the ground states were computed for several structures characterized by different $C_{2'}O_{3'}$ bond lengths and $O_{3'}C_{2'}N_{1'}C_{4'}$ dihedral angles, and at the structures obtained in CI calculations. The values for these geometrical parameters together with the results obtained in the analysis are compiled in Table 5. Shorter CO bond lengths with respect to the standard distance for the peroxo intermediate (1.54 Å), reaching a value as low as 1.20 Å, do not result in changes in the electronic nature of the lowest lying excited state; it maintains a CTIL character. The $\pi_{HOMO} \rightarrow \pi_{LUMO}^*$ excited state becomes progressively closer in energy to the CTIL state, with a minimum energy difference of 0.51 eV for the geometries considered here. Changes in the $O_{3'}C_{2'}N_{1'}C_{4'}$ dihedral angle result in much smaller energy separation and ultimately a change

Table 5. Electronic Transition Character of the Lowest Lying Excited State and Vertical CASPT2 Energies (in eV) between the $\pi_{HOMO} \rightarrow \pi_{CO}^*$ and $\pi_{HOMO} \rightarrow \pi_{LUMO}^*$ States [$\Delta E(S_2-S_1)$] and between the Lowest Lying Excited and Ground States [$\Delta E(S_1-S_0)$] at Different Geometries (see text)[a]

	$C_{2'}O_{3'}$	$O_{3'}C_{2'}N_{1'}C_{4'}$	S_1 nature	ΔE (S_2-S_1)	ΔE (S_1-S_0)
bond	1.30	−125	$\pi_{HOMO} \rightarrow \pi_{CO}^*$	1.03	1.65
	1.28	−125	$\pi_{HOMO} \rightarrow \pi_{CO}^*$	0.93	1.74
	1.26	−125	$\pi_{HOMO} \rightarrow \pi_{CO}^*$	0.83	1.84
	1.24	−125	$\pi_{HOMO} \rightarrow \pi_{CO}^*$	0.72	1.95
	1.22	−125	$\pi_{HOMO} \rightarrow \pi_{CO}^*$	0.62	2.05
	1.20	−125	$\pi_{HOMO} \rightarrow \pi_{CO}^*$	0.51	2.16
dihedral	1.30	−135	$\pi_{HOMO} \rightarrow \pi_{CO}^*$	0.88	1.85
	1.30	−143	$\pi_{HOMO} \rightarrow \pi_{CO}^*$	0.61	2.26
	1.30	−150	$\pi_{HOMO} \rightarrow \pi_{CO}^*$	0.57	2.69
	1.30	−158	$\pi_{HOMO} \rightarrow \pi_{LUMO}^*$	2.14	5.00
CASSCF CI	1.33	−121	$\pi_{HOMO} \rightarrow \pi_{CO}^*$	2.19	0.44
CASPT2 CI	1.32	−119	$\pi_{HOMO} \rightarrow \pi_{CO}^*$	2.47	0.02

[a] Bond lengths and dihedral angles are in Ångstroms and degrees, respectively.

of order (see Table 5). Hence, it is only when the molecule approaches the geometry of the decomposition product [$(S_0)_{min}$]—far from the region of the TS and the CI seam—that the electronic structure of the S_1 state becomes identical to the FS. This region presents a large energy difference between S_1 and the ground state, which indicates that the system is entering the region of the PESs governed by the fluorescence phenomenon.

CI computations at the CASSCF level of theory and including the π system result in a shorter CO bond length (a difference of 0.2 Å) and a similar $O_{3'}C_{2'}N_{1'}C_{4'}$ dihedral angle with respect to the peroxo-like form. Thus, the system still presents sp^3 hybridization and single-bond character of the carbonile group at this point. The electronic nature of the excited state also corresponds to the CTIL excitation. As can be seen in Table 5, strong differential correlation effects characterize the region of degeneracy: the CASPT2 energy difference between the ground and lowest excited states is 0.44 eV at the CI obtained with the CASSCF method. The CASPT2 CI was then computed by means of using the CASSCF gradients (see ref 34 for more details about this computational strategy). The molecule in the region of degeneracy at the CASPT2 level shows a similar geometry to the CASSCF CI point (differences are mainly related to rotations of the methyl group attached to the carbonile moiety) and the same type of excitations between MOs for the lowest excited state. Both CI crossing points have relative energies of 3.51 and 3.36 eV with respect to the $(S_0)_{min}$ equilibrium structure. These energy values must be considered only as an estimation of the CI, since, in contrast to the FS and CS, the molecule in the region of PES crossing is expected to possess the CO_2 part of the peroxo intermediate relatively close to the 2-acetamido-3-methylpyrazine moiety (see, for instance, refs 4 and 14), and therefore the energetic profile might be affected by this leaving group. In order to properly describe this part of the chemiluminescence reaction path, the CO_2 group and relevant MOs in this moiety should be included in the calculations, as was done in previous studies in 1,2-dioxetane,[2] 1,2-dioxetanone,[3] and thiazole-substituted dioxetanone molecules.[4] This is out of the

scope of the present contribution, which is focused on the FS and CS states. A relevant conclusion can still be obtained from the analysis performed here, which supports the use of the peroxo-like form as a starting structure to find the CS: the geometries at the decomposition reaction TS, in its vicinity, and in the region of PES crossing share in common a CTIL excited state and similar structural parameters for the CO moiety.

Subsequent geometry optimizations of the CTIL state of the peroxo-like form in the anion were carried out by using different CASSCF/CASPT2 strategies to determine the chemiluminescence properties and analyze different methodological parameters. First, a small active space (only π orbitals) was used to optimize the structure at the CASSCF level. In the second step, two modifications of the methodology were considered: (1) The lone pair n_O of the oxygen $O_{3'}$ was added since this orbital was shown in previous studies to contribute to the electronic transitions related to the CS, and (2) the dynamical correlation was used to optimize the geometry through the CASPT2 method by using numerical gradients. The results obtained for the VE energies and the selected geometrical parameters to monitor the differences between chemiluminescence and fluorescence are compiled in Tables 3 and 4. The multiconfigurational character of the CS becomes stronger when the n_O orbital is included in the active space. The CTIL and a new excitation from the n_O to the π_{CO}^* orbitals have large contributions in the electronic structure of the CS (see Figure 7). This results in, as a consequence, the elongation of the CO bond length (0.12 Å larger) and a large decrease in the VE (0.87 eV lower). The dihedral angle $O_{3'}C_{2'}N_{1'}C_{4'}$ changes by 7°, and the angle $C_{2'}N_{1'}C_2N_3$ is practically not affected. In the neutral molecule, the $n_O \rightarrow \pi_{CO}^*$ excitation characterizes the lowest excited state, without CTIL contributions. This electronic transition is relevant in the chemiluminescence of molecular systems that do not include any good electron-donating part, for instance, 1,2-dioxetane and dioxetanone.[2,3] Such molecules are much less efficient for chemiluminescence, since the concerted CTIL mechanism does not apply. The second effect studied in the anion, that is, geometry optimizations calculated with the CASPT2 method instead of CASSCF, results in a large stabilization of the CS. The VE is found close to the energy obtained with the big active space (see Table 4). In contrast to the CASSCF geometry optimization, the CASPT2 method provides a structure in which the acetamido part is rotated with respect to the plane of the methylpyrazine group (the dihedral angle $C_{2'}N_{1'}C_2N_3$ is 20°). Much less affected are the CO bond length (0.05 Å larger) and $O_{3'}C_{2'}N_{1'}C_{4'}$ dihedral angle (5° less negative). Interestingly, the CASPT2 geometry optimization of the pure CTIL state results in a CS with a high efficiency of chemiluminescence (f = 0.139). The relative orientation of the acetamido and methylpyrazine parts of the molecule could be the cause for enhancing the emission with respect to the CS_{10in9} structure, since the dihedral angle $C_{2'}N_{1'}C_2N_3$ is larger in CS_{caspt2} and becomes closer to the values found for the $(S_0)_{min}$ and $(S_2)_{min1}$ minima, which show the largest f among all of the structures studied. According to these results, the dihedral angle $C_{2'}N_{1'}C_2N_3$ might be relevant in this molecule to control the interaction between π states. CASPT2(12-in-10) computations at the geometry of the CS_{caspt2} result in a lower f (in particular, f = 0.063), since the $n_O \rightarrow n_{CO}^*$ excitation, which corresponds to a symmetry-forbidden electronic transition, is now contributing to the CS. To analyze the relative contribution of the CTIL and $n_O \rightarrow n_{CO}^*$ excitations in the CS, more accurate CASSCF/CASPT2 studies should be done with small systems in which the concerted CTIL mechanism applies and all of the relevant orbitals of the dioxetanone moiety (see ref 3) as well as those of the π-aromatic system could be included in the active space.

Apart from the differences found in the geometries obtained by means of the mentioned CASSCF/CASPT2 strategies, all of the optimized structures are characterized by CTIL character, a single bond in the CO group (larger CO distances than 1.28 Å) and sp^3 hybridization of the $C_{3'}$ atom (lower absolute values than 132° for the dihedral angle $O_{3'}C_{2'}N_{1'}C_{4'}$). These findings are markedly different from the results obtained in the fluorescence study. While the FS is characterized by a double bond and planar structure for the carbonile group, the single bond CO and sp^3 hybridization of the $C_{3'}$ atom are the main features of the CS. Table 4 also includes data reported in the literature related to the chemiluminescence of 2-methanamidopyrazine,[14] which is a small model of coelenteramide close to the molecule studied in the present work. The structures obtained in that study, by optimizing the first excited state of different conformers at the CIS/6-31+G(d) level of theory, were associated with the light-emitting species of this molecule in the chemiluminescence reaction. However, all of the conformers have CO bond lengths around 1.20 Å, and the $O_{3'}C_{2'}N_{1'}C_{4'}$ dihedral angle is close to 180° (planar conformation of the carbonile group). These results are in agreement with the FS values obtained for the 2-acetamido-3-methylpyrazine anion and largely differ from the CS patterns established in the present work. Regarding the VE energies, larger values (around 3 eV) are found by Isobe et al. for the lowest-excited state optimized structure,[14] which are closer to the FS than the CS present results. Experimentally, the bioluminescence of aequorin and obelin are measured in the ranges 2.19−2.64 and 2.23−3.09 eV,[23] respectively, and the chemiluminescence of coelenteramide seems to have a value of 2.66 eV.[18] On the other hand, the emission maxima in the chemiluminescence spectra of different imidazopyrazinone analogues measured by Hirano et al. are above 2.52 eV.[15] All of these data are larger than the present VE obtained with the most accurate strategies CASSCF(12-in-10) and CASPT2. As explained in the absorption and fluorescence analysis, the remaining part of the coelenteramide molecule that is not present in 2-acetamido-3-methylpyrazine, mainly the phenolate ring, will contribute to enlarge the energy separation between the CS and ground states. In agreement with the present theoretical findings, the data obtained by Hirano et al. show in all cases larger emission maxima for the fluorescence process with respect to chemiluminescence.[15]

Finally, according to the findings of our computations and the associated analysis, some recommendations can be made for theoretical and experimental studies on chemiluminescence. Reliable theoretical studies on the chemiluminescence properties of light-emitting species should not be performed in general by using the ground-state equilibrium structure of the chemiluminescence product as the starting point to find the CS, since different excited state structures may be found for the FS and CS, as shown in the present work. Instead, the whole chemiluminescence reaction must be modeled, from the peroxo precursor to the formation of the emissive state, or the CS can be reached by carrying out geometry optimizations from a structure close to the peroxo intermediate. Regarding the experiments, procedures analyzing the luminescence emitted by the reaction product after irradiation should be avoided in favor of techniques that involve carrying out the whole chemiluminescence reaction and the analysis of the radiation produced. The differences between the

CS and FS might become even stronger in large systems, since the complexity of the PESs increases along with the number of internal degrees of freedom, and therefore the relative positions of the CS and FS states on the excited state surface could differ substantially.

CONCLUSIONS

The characterization of the chemiluminescence and fluorescence states of a small model for the coelenteramide and *Cypridina* oxyluciferin systems, in particular, the 2-acetamido-3-methylpyrazine anion molecule, has been carried out by means of the CASSCF/CASPT2 method in order to establish the molecular basis of the differences between both luminescent phenomena. The neutral form of the molecule has been also considered in some parts of the study, since this protonated form could be also relevant in the chemiluminescence process. In the Franck−Condon region of the ground-state equilibrium structures, the lowest excited states correspond to excitations between orbitals delocalized over the π-conjugated system, while electronic transitions to the carbonile moiety, which are related to the concerted CTIL mechanism responsible for an efficient chemiluminescence process, are found to be very high in energy (above 7 eV, which is more than 2 eV higher in energy with respect to the brightest transitions). In contrast, the CTIL state has been obtained as the lowest-lying excited state of the anion when a geometry close to the peroxo intermediate of the chemiluminescence reaction is used. Therefore, this strategy seems to be more appropriate for finding the CTIL transition and has been employed to characterize the CS. The results obtained for the neutral form by using the same procedure are different: none of the lowest excited states correspond to a CTIL transition. Thus, the anion form is the relevant species for the efficient chemiluminescence of 2-acetamido-3-methylpyrazine, which is consistent with the fact that this deprotonated system has a better activator group (with low ionization potential) for turning on the concerted CTIL mechanism. The protonated species cannot be discarded, however, as the light-emitting molecule in different imidazopyrazinone derivatives in which other chemical groups of the system can act as activator groups, as has been proved elsewhere.[12,15] In addition, the protonation state of the $N_{1'}$ atom will depend on the closest amino acids of the apoprotein in the bioluminescence process, and the substrate−apoprotein interactions must be analyzed to ultimately understand the role of the protonated/deprotonated species in the chemiluminescence taking place in living organisms. The present photochemical study of the anion molecule has led to three structures which contribute to the fluorescent properties of the molecule: two shallow minima on the S_2 surface and a minimum in the S_1 surface, with VEs of 3.59, 2.21, and 2.11 eV, respectively. The deactivation of the brightest state of the anion molecule is guided by a rotation of the acetamido moiety with respect to the plane of the methylpyrazine part, which reaches a perpendicular conformation at the CI between the S_1 and S_2 surfaces. All of the emissive states found for the anion and neutral systems are characterized by a planar structure (sp^2 hybridization) and double bond of the CO, which do not differ much from the properties of the carbonile group in the ground-state equilibrium minimum. In the analysis of the CS for the anion, distinct multiconfigurational approaches have been employed, finding decreases of the VE when the oxygen lone pair of the CO chemical group is included in the active space and when dynamical correlation is included in the CASPT2 geometry optimizations. According to these results, the chemiluminescent emission of 2-acetamido-3-methylpyrazine is lower in energy than fluorescence, the most accurate obtained values being in the range 1.60−1.72 eV. All levels of theory result in an out-of-plane conformation of the CO group (sp^3 hybridization) with a large bond length (single bond character), which have been established as the structural patterns of the chemiluminescence phenomenon. The comparison of the results obtained in the fluorescence and chemiluminescence analysis shows significant differences in the electronic structure and geometrical parameters of the CS and FS states for the 2-acetamido-3-methylpyrazine molecule, which must be taken into account in the design of future theoretical and experimental studies on bioluminescence and chemiluminescence. In the light of the present findings, we do not recommend, in general, procedures in which the properties of the chemiluminescent state are obtained by using the ground-state equilibrium structure of the reaction product, unless a previous analysis supporting this strategy had been carried out. A much safer computational approach is to start with a structure close to the peroxo intermediate of the chemical reaction in order to characterize the CS.

ASSOCIATED CONTENT

Supporting Information. Complete sets of CASSCF orbitals of 2-acetamido-3-methylpyrazine anion and neutral molecules are presented in Figures S1 and S2, respectively. The CASSCF MEPs related to the Figures 4 and 5 and corresponding to the MEP of the S_2 state from $(S_0)_{min}$, in the first case, and the MEP of the S_1 state from the CI, in the latter, are displayed in Figures S3 and S4, respectively. Additional MEPs on the S_1 surface are also provided: Figures S5−S8 show the CASSCF MEP from the $(S_2)_{min1}$, the CASPT2//CASSCF MEP from the $(S_2)_{min1}$, the CASSCF MEP from the $(S_0)_{min}$, and the CASPT2//CASSCF MEP from the $(S_0)_{min}$, respectively. The coordinates for the main structures of the present study can be found in Table S1. This material is available free of charge via the Internet at http://pubs.acs.org.

AUTHOR INFORMATION

Corresponding Author

*E-mail: Daniel.Roca@kvac.uu.se, Roland.Lindh@kvac.uu.se.

Notes

The authors declare no competing financial interest.

ACKNOWLEDGMENT

D.R.-S. thanks the European Research Council under the European Community's Seventh Framework Programme (FP7/2007-2013)/ERC grant agreements no. 255363. I.N. thanks Prof H. M. Marques for funding through the DST/NRF SARChI initiative. Y.-J.L. thanks the National Nature Science Foundation of China. N.F. thanks the French National Center for Scientific Research. R.L. thanks the Swedish Research Council for financial support.

REFERENCES

(1) Nic., M.; Jirat, J.; Kosata, B. *IUPAC. Compendium of Chemical Terminology*, 2nd ed. (the "Gold Book"). http://goldbook.iupac.org

(accessed Sep 6, 2011). Compiled by McNaught, A. D.; Wilkinson, A. Blackwell Scientific Publications: Oxford, U. K., 1997. Updates compiled by Jenkins, A. ISBN 0-9678550-9-8. DOI: 10.1351/goldbook.

(2) De Vico, L.; Liu, Y. J.; Krogh, J. W.; Lindh, R. *J. Phys. Chem. A.* **2007**, *111*, 8013–8019.

(3) Liu, F.; Liu, Y. J.; De Vico, L.; Lindh, R. *J. Am. Chem. Soc.* **2009**, *131*, 6181–6188.

(4) Liu, F. Y.; Liu, Y. J.; De Vico, L.; Lindh, R. *Chem. Phys. Lett.* **2009**, *484*, 69–75.

(5) Navizet, I.; Liu, Y.-J.; Ferré, N.; Roca-Sanjuán, D.; Lindh, R. *Chem. Phys. Chem.* **2011**, DOI: 10.1002/cphc.201100504.

(6) Seliger, H. H.; McElroy, W. D. *Arch. Biochem. Biophys.* **1960**, *88*, 136–141.

(7) Hawronskyj, J. M.; Holah, J. *Trends Food Sci. Tech.* **1997**, *8*, 79–84.

(8) Lang, T.; Goyard, S.; Lebastard, M.; Milon, G. *Cell. Microbiol.* **2005**, *7*, 383–392.

(9) Gundermann, K.-D. *Chemilumineszenz Organischer Verbindungen*; Springer: Berlin, 1968; pp 1−174.

(10) Gundermann, K.-D. In *Photochemistry. Topics in Current Chemistry*; Boschke, F., Ed.; Springer-Verlag: New York, 1974; Vol. 46; pp 61−139.

(11) *Bioluminescence & Chemiluminescence: Progress and perspectives*, Proceedings of the 13th International Symposium Pacifico Yokihama, Japan, August 2−6; Tsuji, A., Matsumoto, M., Maeda, M., Kricka, L. J., Stanley, P. E., Eds.; World Scientific: Singapore, 2004.

(12) Isobe, H.; Takano, Y.; Okumura, M.; Kuramitsu, S.; Yamaguchi, K. *J. Am. Chem. Soc.* **2005**, *127*, 8667–8679.

(13) Roca-Sanjuán, D.; Aquilante, F.; Lindh, R. *WIREs Comp. Mol. Sci.* **2011**, DOI: 10.1002/wcms.97.

(14) Isobe, H.; Yamanaka, S.; Kuramitsu, S.; Yamaguchi, K. *J. Am. Chem. Soc.* **2008**, *130*, 132–149.

(15) Hirano, T.; Takahashi, Y.; Kondo, H.; Maki, S.; Kojima, S.; Ikeda, H.; Niwa, H. *Photochem. Photobiol. Sci.* **2008**, *7*, 197–207.

(16) Imai, Y.; Shibata, T.; Maki, S.; Niwa, H.; Ohashi, M.; Hirano, T. *J Photochem. Photobiol. A.* **2001**, *146*, 95–107.

(17) Mori, K.; Maki, S.; Niwa, H.; Ikeda, H.; Hirano, T. *Tetrahedron.* **2006**, *62*, 6272–6288.

(18) Shimomura, O.; Teranishi, K. *Luminescence* **2000**, *15*, 51–58.

(19) Hirano, T.; Ohmiya, Y.; Maki, S.; Niwa, H.; Ohashi, M. *Tetrahedron Lett.* **1998**, *39*, 5541–5544.

(20) Wu, C.; Nakamura, H.; Murai, A.; Shimomura, O. *Tetrahedron Lett.* **2001**, *42*, 2997–3000.

(21) Fujimori, K; Komiyama, T.; Tabata, H.; Nojima, T.; Ishiguro, K.; Sawaki, Y.; Tatsuzawa, H.; Nakano, M. *Photochem. Photobiol.* **1998**, *68*, 143–149.

(22) Stepanyuk, G. A.; Golz, S.; Markova, S. V.; Frank, L. A.; Lee, J.; Vysotski, E. S. *FEBS Lett.* **2005**, *579*, 1008–1014.

(23) Belogurova, N. V.; Kudryasheva, N. S.; Alieva, R. R.; Sizykh, A. G. *J Photochem. Photobiol. B.* **2008**, *92*, 117–122.

(24) Shimomura, O.; Johnson, F. H.; Saiga, Y. *J. Cell. Comp. Physiol.* **1962**, *59*, 223–240.

(25) Morin, J. G.; Hastings, J. W. *J. Cell. Physiol.* **1971**, *77*, 305–312.

(26) Shimomura, O.; Jonhson, F. H.; Masugi, T. *Science* **1969**, *164*, 1299–1300.

(27) Liu, Z. J.; Stepanyuk, G. A.; Vysotski, E. S.; Lee, J.; Markova, S. V.; Malikova, N. P.; Wang, B. C. *Proc. Natl. Acad. Sci. U.S.A.* **2006**, *103*, 2570–2575.

(28) Roos, B. O.; Lindh, R.; Malmqvist, P.-Å.; Veryazov, V.; Widmark, P.-O. *J. Phys. Chem. A.* **2004**, *108*, 2851–2858.

(29) Andersson, K.; Malmqvist, P.-Å.; Roos, B. O. *J. Chem. Phys.* **1992**, *96*, 1218–1226.

(30) De Vico, L.; Olivucci, M.; Lindh, R. *J. Chem. Theory Comput.* **2005**, *1*, 1029–1037.

(31) Aquilante, F.; De Vico, L.; Ferré, N.; Ghigo, G.; Malmqvist, P.-Å.; Neogrády, P.; Pedersen, T. B.; Pitoňák, M.; Reiher, M.; Roos, B. O.; Serrano-Andrés, L.; Urban, M.; Veryazov, V.; Lindh, R. *J. Comput. Chem.* **2010**, *31*, 224–247.

(32) González-Ramírez, I.; Roca-Sanjuán, D.; Climent, T.; Serrano-Pérez, J. J.; Merchán, M.; Serrano-Andrés, L. *Theor. Chem. Acc.* **2011**, *128*, 705–711.

(33) Bernardi, F.; Olivucci, M; Robb, M. A. *Pure Appl. Chem.* **1995**, *67*, 783–789.

(34) Roca-Sanjuán, D.; Olaso-González, G.; González-Ramírez, I.; Serrano-Andrés, L.; Merchán, M. *J. Am. Chem. Soc.* **2008**, *130*, 10768–10779.